Macromolecules

pubs.acs.org/Macromolecules Article

Linear Viscoelastic Response of Comb/Linear Polymer Blends: A Three-Step Relaxation Process

Zhi-Chao Yan,* Evelyne van Ruymbeke, and Dimitris Vlassopoulos

Cite This: *Macromolecules* 2021, 54, 11047−11060 Read Online

ACCESS | Metrics & More | Article Recommendations

Downloaded via UNIV CATHOLIQUE DE LOUVAIN on January 30, 2022 at 14:20:36 (UTC).
See https://pubs.acs.org/sharingguidelines for options on how to legitimately share published articles.

ABSTRACT: This study addresses the linear viscoelasticity of blends involving monodisperse comb and linear polymers, the latter being the matrix of varying molar mass. This is dynamically a three-component system, comprising linear chains, branches (which are short enough to undergo essentially Rouse relaxation), and backbones. We examine systematically the relaxation of the same comb diluted in the linear matrix as a function of the molar mass of the linear chain for all possible situations (when the latter is oligomer or polymer relaxing faster or slower than the branches) as well as the case of backbone self-entanglements. We develop a simple tube model for the contributions of the three components to comb relaxation by accounting for the dynamic dilution and two delay factors, one for the matrix and another for the comb. The former represents the frictional contribution of the linear polymers to the constraint release Rouse process of the branches and backbone, and the latter represents the relevant effect of the branches on the backbone motion. The model provides an excellent quantitative description of the experimental data. The resulting retardation factors controlling the relaxation process of the combs as a function of the linear polymer's molar mass complement and extend our earlier investigations with blends involving H-polymers in linear matrices, pointing toward a universal description of the dynamic response of architecturally complex polymers in linear matrices based on constraint release mechanisms. This finding enhances our ability to tailor the dynamics of topological homopolymer blends as per our wish. The remaining challenges associated with the possible universality of the delay factor of combs and the coupling of branch and backbone motion are discussed.

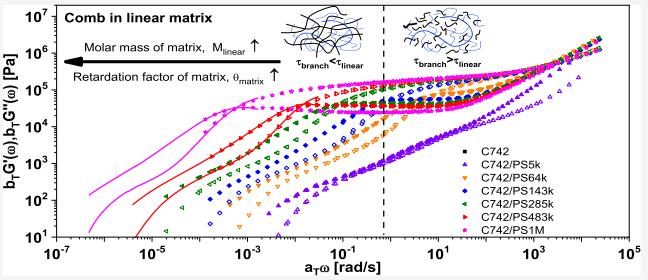

1. INTRODUCTION

The tube model[1,2] has successfully established a relationship between topology of entangled polymers and their rheological properties. The linear viscoelasticity (LVE) of monodisperse entangled linear polymers was first well understood and predicted by means of state of the art tube-based molecular models.[3−6] The LVE of complex topological polymers, such as comb and H-polymers, is also understood in the context of a tube-model-based hierarchical relaxation picture, according to which the branches relax by retraction first and then the backbone reptates in a solvent-like environment diluted by relaxed branches.[7−18] With this background, investigating the dynamics of topological blends and in particular, understanding how such an architecturally complex macromolecule (which mimics commercial polymers) relaxes when diluted in a linear matrix, has been an important research direction.

So far, the study of the rheological behavior of binary blends has focused mainly on star/linear blends[19−25] or on linear/linear blends.[4,26−40] Determining the terminal relaxation of the slower component is a nontrivial challenge. The competition between a single-chain relaxation mechanism, for example, reptation and contour length fluctuation (CLF) in a fixed environment, and the relaxation triggered by the motion of the surrounding chains, for example, by constraint release (CR), constitutes the main complexity of this problem.[19−42] A criterion marking the crossover from the relaxation of the slow component in a well-entangled environment (*i.e.,* accounting for the entanglements with both short and long components) to a CR-dominated relaxation was first suggested by Struglinski and Graessley[26] based on the ratio of the reptation time of the long chains in an non-dilated tube and their CR Rouse (CRR) time, which yields $s_{SG} = Z_{long}/Z_{linear}^3$, with Z the number of nondilated entanglements and subscripts long and linear representing long and short chains in blends, respectively. The critical transition ratio, $s_{SG,c}$, was experimentally found to be around 0.1 in binary linear blends.[4,28,40,41] Low M_w components behave like solvents only when s_{SG} is larger than this value. In star/linear blends with star as the slow components, $s_{SG,c}$ has been approximated to around 0.075.[29] Viovy *et al.*[30] and, more recently, Read *et al.*[40] extended the SG criteria by incorporating

Received: June 20, 2021
Revised: October 25, 2021
Published: November 19, 2021

ACS Publications © 2021 American Chemical Society

the concentration of long chains. In their dynamic diagram indicating regimes of different mechanisms of relaxation, there are two distinct types of entanglements: a thin tube in which long chains entangle with all other chains and a fat tube in which long chains only entangle with other long chains (Figure 1).[24,30,39,40] The time that the long component needs to explore its fat tube depends on both the diameter of the fat tube (*i.e.*, on the concentration of the slow component) and on how fast the short component disentangles and re-entangles (*i.e.*, on its relaxation time).[37,40] The transition from the thin tube picture to the fat tube picture is well described by a CRR process, that is, a Rouse process governed by the disentanglement dynamics of the short component.[18,24,25,29]

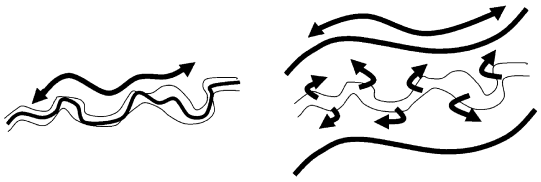

Figure 1. Cartoons depicting the entanglement of long chains in binary linear/linear blends: long chains entangle with all other chains and reptate along a thin tube (left) *vs* long chains only entangle with other long chains and reptate along a fat tube driven by CR (right).

When the long chains are much longer than the short chains, the CR effect from the latter is the dominant reason for long chain relaxation, and the full dynamic tube dilution (full-DTD) picture[31,38,40] can be used as soon as the long chains have explored their large tube. If the long component is self-entangled, it has been recently proposed that the motion of the long chains along the contour of the thin tube is accelerated by the enhanced CLF effect due to CR in the fat tube.[25,37,38,40,43] Otherwise, if the long component is diluted in the linear matrix and does not contain self-entanglements, the fat tube does not exist and its relaxation is fully governed by the CRR process. Its terminal relaxation time, $\tau_{CRRlong}$, is therefore well described as[25,26,40]

$$\tau_{CRRlong} = \tau_{obs} Z_{long}^{\ 2} = \theta_{matrix} \tau_e Z_{long}^{\ 2} \quad (1)$$

where τ_{obs} represents the lifetime of an entanglement between a short and a long component and τ_e represents the intrinsic Rouse time of an entanglement segment. The CRR time $\tau_{CRRlong}$ is thus longer than the intrinsic Rouse time, $\tau_R = \tau_e Z_{long}^{\ 2}$, by a factor $\theta_{matrix} \geq 1$. While according to Graessley and Struglinski[26] τ_{obs} should be well-described by the disentanglement time of the polymer matrix, τ_{linear}, recent works have shown that it is actually much smaller.[38,40] In particular, based on slip-spring simulations on bidisperse linear blends, Read *et al.*[40] found that τ_{obs} is well determined by the empirical relationship

$$\tau_{obs}(\text{slip-spring}) = 0.047\tau_{linear}\left(1 + \frac{1}{0.36\sqrt{\frac{\tau_e}{0.047\tau_{linear}}}}\right) + \tau_e \quad (2)$$

On the other hand, Shahid *et al.* proposed that for linear chains diluted in a short linear matrix, this time can be approximated as[38]

$$\tau_{obs} = \max\left(\tau_e, \frac{\tau_{linear}}{Z_{linear}^{\ 2}}\right) \quad (3)$$

based on the idea that the reptation of the linear short chains leads to the disentanglement of Z_{linear} obstacles. Similar results were reported by Ebrahimi *et al.*[25] for the case of star polymers diluted in a linear matrix. While eqs 2 and 3 yield very similar results if the linear matrix is not too entangled ($Z_{linear} < 10$), they largely differ if longer matrices are used.[44] However, these equations were not tested in this regime, which is difficult to reach experimentally.

For more complex topological blends, such as comb polymers diluted in a linear matrix, the challenge lies in the fact that the blends are actually behaving as dynamically three-component blends, including linear chains, branches, and backbones. While both the linear matrix and the branches control the eventual relaxation of the macromolecular backbone, the relaxation of the branches is controlled by the motion of the linear chains if the latter are short enough to relax first. On the other hand, if the comb is diluted in a very long linear matrix, the branches are expected to relax in an undiluted thin tube, and the relaxation of the comb backbone should depend on the motion of both the branches and the linear matrix. As illustrated in Figure 2, there are therefore three successive levels of relaxation (linear chains *vs* branches *vs* backbone), which strongly depend on the respective molar masses and the composition of the blend.

Recently, we investigated the viscoelastic properties of a H-polymer diluted in linear matrices of different molar masses and concentration.[44] When diluted in an oligomeric matrix at concentration low enough to avoid self-entanglements, it was found that the terminal relaxation of the H backbone was well described by a Rouse process, but with a delay θ_H due to the extra friction coming from the branches attached to the backbone. By diluting the H-polymer at the same concentration in a longer (entangled) linear matrix which still relaxes much faster than the branches of the H-polymer, the relaxation of the branches was well described by a CRR process, that is, by considering that their intrinsic Rouse relaxation was delayed by a factor $\theta_{matrix} > 1$, as described by eq 1. On the other hand, it was found that the CRR relaxation of the H backbone was well described by considering a retardation factor equal to the product $\theta_H\theta_{matrix}$, that is, by accounting for the extra friction coming from the branches, on top of the overall delay is the

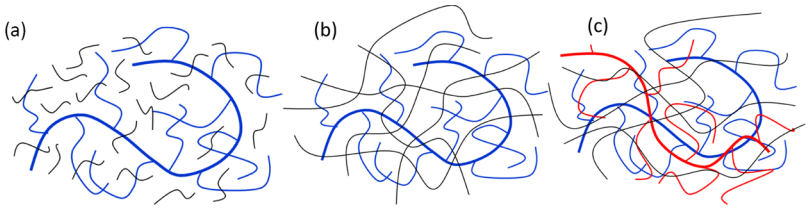

Figure 2. Cartoon of (a) combs in a sea of short linear chains, (b) combs in a sea of long entangled linear chains, and (c) combs that entangle with themselves and with a linear matrix. The blue and red cartoons are combs, while the black ones are linear chains.

https://doi.org/10.1021/acs.macromol.1c01329
Macromolecules 2021, 54, 11047−11060

linear matrix during its Rouse relaxation. While the delay factor attributed to the linear matrix θ_{matrix} depends on its molar mass, the delay factor coming from the H branches, θ_H, is constant. This interesting result suggests that one can decouple the effects of the two contributions (matrix and branches) to determine the terminal relaxation time of the H backbone. However, because only one architecture (and in fact one H-polymer sample only) was tested, the validity of this result, let alone its potential dynamic implications, could not be assessed.

In this work, we build-up on our earlier work[44] and investigate the relaxation dynamics of a (more complex) comb polymer[11,13,45−47] diluted in different linear matrices (same as in ref 44) encompassing the three situations, as shown in Figure 2. The following specific challenges are addressed:

(i) Because the same linear polymers are used as in ref 44, we would like to examine whether the same delay factor θ_{matrix} can be used to determine the CRR of the comb's branches. Furthermore, we would like to know whether the influence of the extra friction due to the branches on the relaxation of the backbone can be taken into account by means of a single parameter, θ_{comb}, and whether it depends on the molar mass of the linear matrix. This may provide a new tool to tailor the flow properties of architecturally complex polymers.

(ii) In addition, we explore the relaxation of the comb backbone in very long linear matrices. In such a situation, the branches of the comb are expected to relax before the relaxation time of the linear chains by retraction in a thin tube (rather than by CRR process). The effects of inverting the relaxation order of the branches and the linear matrix and their consequences on the motion of the comb backbone are not known and will be assessed. In particular, it is interesting to examine whether the overall delay of the backbone CRR relaxation can still be rationalized by the product $\theta_{comb}\theta_{matrix}$. In our earlier work with H/linear polymer blends,[44] this regime could not be examined unambiguously due to the fact that the backbone and the branches of the H-polymer had almost the same molar mass;[48] hence, the dynamics could not be clearly distinguished. In the present work, we use a comb polymer with a long backbone and multiple much shorter branches; hence, the two relaxation processes are decoupled.[11] Furthermore, the analysis should allow us to determine the molar mass dependence of θ_{matrix} in case of very long linear chains and therefore to discriminate between eqs 2 and 3.

This article is structured as follows. We first describe the materials used, their characteristics, and the experimental methods. Then, the model developed to predict the viscoelastic properties of the different blends is presented. In Section 4, the LVE data are discussed with emphasis on the systematic examination of their dependence on concentration and molar mass of linear chains. The data are analyzed in the context of the model in Section 5. Finally, Section 6 presents the concluding remarks.

2. MATERIALS AND METHODS

2.1. Polymers. The comb polymer, C742, is a polystyrene (PS) consisting of a linear, monodisperse backbone with a weight-average molar mass M_{BB} of 860 kg/mol, on which an average of $q = 29$ nearly monodisperse linear branches with a number-average molar mass M_{branch} of 47 kg/mol are randomly grafted. Both backbones and branches have a polydispersity index M_w/M_n smaller than 1.07.[11,13,45,46] It was synthesized anionically and extensively characterized by Roovers.[45,47] Whereas grafting is random, based on the synthesis, characterization, and rheological analysis, we can reasonably consider that we have nearly equidistant branches.[11] Recently, this sample has been characterized again by gel permeation chromatography and temperature-gradient interaction chromatography[46] and rheology[11] to confirm the molar mass distribution, molecular structure, and stability over long time. The monodisperse ($M_w/M_n < 1.05$) linear samples are PS5k, PS64k, PS143k, PS285k, PS483k, and PS1M, with the code denoting the weight average molar mass and units k for kg/mol and M for 10^3 kg/mol (see Table 1). They were obtained either from Polymer Laboratories (USA) or from Polymer Source (Canada). Blends were prepared using an excess of toluene as co-solvent. After complete dissolution, the co-solvent was first slowly evaporated at room temperature and then more rapidly at elevated temperatures above the glass transition temperature in a vacuum oven. In order to ensure that toluene was completely removed, the weight of the blends was monitored. All blends (code C742/PSXk) have the same volume concentration of the comb ν_{comb} of 0.17, except for C742/PS143k for which $\nu_{comb} = 0.5$. The number of entanglements Z_{BB}, Z_{branch}, and Z_{linear} are defined as M_{BB}/M_e, M_{branch}/M_e, and M_{linear}/M_e for backbone, branches, and linear chains, respectively. M_e is the molar mass between entanglements in the melt and has a value of 14.8 kg/mol, consistent with our previous work. The main molecular characteristics are listed in Tables 1 and 2.

Table 1. Weight-Average Molar Mass and Relaxation Time (160 °C) of Linear Polymers

	M_w (kg/mol)	$\tau_{c,linear}$ [a] (s)	T_g (°C)[b]
PS5k	5		87.6
PS64k	64	0.053	104
PS143k	143	0.70	106
PS285k	285	10	106
PS483k	483	53	106
PS1M	1000	1.0×10^3	107

[a]Determined from the crossover of G' and G''. [b]Obtained from ref 44.

2.2. Methods. Rheological measurements were performed on a strain-controlled ARES rheometer (TA Instruments, USA), equipped with a force rebalance transducer (2KFRTN1) and a forced convection oven to enable accurate temperature control (±0.1 °C) in nitrogen environment. Both linear dynamic frequency sweep and nonlinear step-rate measurements were performed in a home-made cone partitioned-plate geometry geometry, which was designed to minimize the flow instabilities like edge fracture and wall slip.[49,50] In this study, we only discuss the LVE response. For the top geometry, a home-made stainless steel plate with 6 mm diameter was used along with a shaft (outer ring) of inner diameter 10 mm, allowing the entire geometry to fit into the ARES convection oven.[46] For the bottom geometry, a standard 25 mm diameter cone with an angle of 0.1 rad and a truncation of 0.051 mm was used. For C742/PS483k and C742/PS1M, the relaxation time is too long to be probed by dynamic frequency sweeps at low enough temperatures in the absence of degradation. Hence, we resorted to creep measurements at 170 °C using a stress-controlled Physica MCR 501 (Anton Paar, Austria) rheometer. For C742/PS483k, a stress of 150 Pa was applied during 2.4×10^5 s. For C742/PS1M, a stress of 300 Pa was applied during 5.7×10^5 s. It was checked that the applied stresses were within the LVE regime, while the measurement times were chosen so that the terminal regime could be reached. After completing the creep measurements, dynamic frequency sweeps were performed and the moduli were found to overlap with those measured before creep. The compliance data as a function of time were subsequently converted to the dynamic storage and loss moduli G' and G'' as a function of angular frequency. The details of conversion are discussed in ref 51. The converted data extend the moduli to lower frequencies, while they overlap with the conventional dynamic frequency sweep data from ARES (see Section 4 below).

https://doi.org/10.1021/acs.macromol.1c01329
Macromolecules 2021, 54, 11047−11060

Table 2. Molecular Characteristics of the Investigated Polymers and Comb−Linear Blends

	ν_{comb}	M_{BB} (kg/mol)	M_{branch} (kg/mol)	ν_{BB}[a]	$M_{e,BB}$ (kg/mol)[b]
C742[c]	1	860	47 (q = 29)	0.36	41
C742/PS5k	0.17			0.06	245
C742/PS64k	0.17			0.06	245
C742/PS143k	0.17			0.06	245
C742/PS143k	0.50			0.18	82
C742/PS285k	0.17			0.06	245
C742/PS483k	0.17			0.06	245
C742/PS1M	0.17			0.06	245

[a]Equal to $\frac{\frac{28}{30}M_{BB}}{M_{BB}+29M_{br}}\nu_{comb}$. [b]Equal to M_e/ν_{BB}. [c]T_g is 106 °C.[44]

3. MODELING

In order to model the LVE properties of the comb/linear blends, we first determine the stress relaxation modulus as a function of time, $G(t)$, taking into account the contribution from the linear matrix, the branches, and the backbone of the comb[15,44]

$$G(t) = \nu_{linear}G_{linear}(t) + \nu_{branch}G_{branch}(t) + \nu_{BB}G_{BB}(t) \quad (4)$$

where ν_{linear}, ν_{branch}, and ν_{BB} are the weight fractions of the linear matrix, the branch, and the backbone, respectively. Then, the storage and loss moduli are determined based on the approximation of Schwarzl.[51] While usually with linear/linear or star/linear blends the total fraction of unrelaxed tube segments is first determined and then used to determine the CR effect, here we shall consider each of the three dynamic constituents above separately in order to be able to properly account for the different relaxation processes.

3.1. Relaxation of the Linear Matrix. If the linear matrix is unentangled, its contribution to the relaxation modulus can be approximated by the intrinsic Rouse relaxation[1,18,44]

$$G_{linear}(t) = \frac{\rho RT}{M_{linear}}\sum_{p=1}^{p=N}\exp\left(\frac{-2p^2}{\tau_R(M_{linear})}\right) \quad (5)$$

Otherwise, its relaxation modulus includes the fast Rouse relaxation taking place up to the time for relaxation of the entanglement segments, followed by its disentanglement process by CLFs and by reptation[3]

$$G_{linear}(t) = G_{R,linear}(t) + G_{d,linear}(t) \quad (6)$$

with

$$G_{R,linear}(t) = \frac{\rho RT}{M_{linear}}\left\{\frac{1}{4}\sum_{p=1}^{Z_{linear}}\exp\left(\frac{-p^2t}{\tau_R(M_{linear})}\right) + \sum_{p=Z_{linear}+1}^{n}\exp\left(\frac{-2p^2t}{\tau_R(M_{linear})}\right)\right\} \quad (7)$$

and

$$G_{d,linear}(t) = G_N^0\varphi_{linear}(t)\phi(t)^{\alpha} \quad (8)$$

where G_N^0 is the entanglement plateau modulus. It is related to the molar mass between two entanglements, M_e, by the relationship[52]

$$G_N^0 = \frac{4}{5}\frac{\rho RT}{M_e} \quad (9)$$

The value of G_N^0 was fixed to 0.23 MPa, consistent with ref 44, which is close to the usual value proposed in literature, 0.20 MPa. The value of M_e was fixed to 14.8 kg/mol. The dynamic dilution exponent α has been fixed to 1, in agreement with refs 36 37 44,. It must be noted here that previous research studies have suggested that while α = 1, the effective dilation exponent determined from the experimental data (by looking at the decrease of the storage modulus) may be larger than unity (≈1.3) at long time.[36,53] This increased effect of dilution has been attributed to the possible monomeric tension equilibration along the slow component, dictated by the motions of the short component. In the present work, we do not account for this extra process. Indeed, its influence is negligible in the relaxation of the short component (see eq 8), which takes place at a short time. Furthermore, for most of the comb/linear blends, the comb polymer is relaxed by the Rouse or CRR process, and consequently, the dilution exponent has no influence because the dilated tube does not exist anymore. However, as further discussed in Section 5.6, omitting this process could slightly influence the survival fraction of initial backbone−backbone entanglement segments in case the comb backbones are self-entangled.

In eq 8, the unrelaxed fraction of initial tube segments at time t, $\varphi_{linear}(t)$, is determined by considering all molecular segments along the chain and determining the probability $p_{rept}(x,t)$ that they are not relaxed by reptation at time t and the probability $p_{fluc}(x,t)$ that they are not relaxed by CLF[15]

$$\varphi_{linear}(t) = \int_{x=0}^{x=1} p_{rept}(x,t)p_{fluc}(x,t)\mathrm{d}x \quad (10)$$

where x is a normalized curvilinear variable that represents primitive path segments along a given arm, measured as a fractional distance along the branch inward from the free end (note that linear chains are treated like star polymers with two arms.) The probability $p_{rept}(x,t)$ of a segment at the fractional distance of x to survive from the reptation process at time t is given by the Doi−Edwards equation,[1] while the survival probability from the fluctuation process is approximated by the decreasing exponential function, $\exp(-t/\tau_{fluc}(x))$, where $\tau_{fluc}(x)$ is the fluctuations time corresponding to segment at the position of x, as described in ref 54. The unrelaxed fraction for the branches on the comb, $\varphi_{branch}(t)$, uses the same formula of eq 10, with $p_{fluc}(x,t) = \exp(-t/\tau_{fluc}(x))$, where $\tau_{fluc}(x)$ is described in ref 54, and $p_{rept}(x,t) = 1$ considering no reptation for branches.

On the other hand, the tube dilation factor $\phi(t)$ takes into account the effect of CR on the chain entanglements and defines the diameter of the dilated tube (such as $a = a_0\phi(t)^{-\alpha/2}$). It can be approximated by the overall unrelaxed fraction of initial tube segments

https://doi.org/10.1021/acs.macromol.1c01329
Macromolecules 2021, 54, 11047−11060

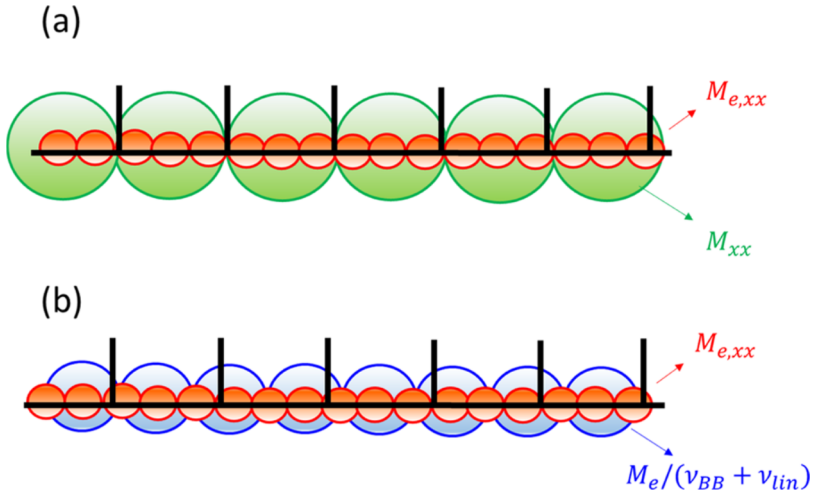

Figure 3. Rouse and CRR modes of the comb backbone when (a) the linear matrix relaxes faster than the branches and (b) the branches relax faster than the linear matrix.

$$\phi(t) = \nu_{\text{linear}}\varphi_{\text{linear}}(t) + \nu_{\text{branch}}\varphi_{\text{branch}}(t) + \nu_{\text{BB}} \text{ for } t < \tau_{\text{BB}} \tag{11}$$

In eq 11, it is assumed the inner comb backbone does not relax at the time scale at which the linear matrix and the comb branches relax. Note that the outer branches of the backbone are taken into account in the fraction ν_{branch}, with the "backbone" representing only the inner part of the main chain.

3.2. Relaxation of Branches. Each branch of the polymer comb C742 contains three entanglements. Therefore, if their relaxation is faster or of the order of the relaxation time of the linear matrix, the branches mainly relax by CLFs or arm retraction, from $x = 0$ at the extremity to $x = 1$ at the branching point to which they are attached.[55] As for the linear matrix, CR must also be accounted for.[56] Thus, in this case, their relaxation is described by eqs 5−11, where the branches are not allowed to reptate [*i.e.*, fixing $p_{\text{rept}}(x,t) = 1$].

However, if the branches relax slower than the linear matrix, they will rather relax by Rouse and CRR processes because they do not contain self-entanglements.[44] In such a case, the molecular segments of mass shorter than M_e relax by intrinsic Rouse process, while the relaxation of the longest segments, that is, the longest modes of the branches, has to include the extra friction coming from the disentanglement/re-entanglement of the matrix.[25] This is done by considering a delay factor θ_{matrix}. Therefore, following ref 14, we have

$$G_{\text{branch}}(t) = \frac{\rho RT}{2M_{\text{branch}}}\left(\sum_{p=1}^{p=Z_{\text{branch}}} \exp\left(\frac{-2p^2}{\theta_{\text{matrix}}\tau_R(2M_{\text{branch}})}\right) + \sum_{p=Z_{\text{branch}}+1}^{p=N} \exp\left(\frac{-2p^2}{\tau_R(2M_{\text{branch}})}\right)\right) \tag{12}$$

If the linear matrix comprises oligomers and if the weight fraction of the comb polymer is 0.17 (see Table 2), the comb branches are not entangled anymore and they fully relax by an intrinsic Rouse process

$$G_{\text{branch}}(t) = \frac{\rho RT}{2M_{\text{branch}}}\sum_{p=2}^{p=2N} \exp\left(\frac{-2p^2}{\tau_R(2M_{\text{branch}})}\right) \tag{13}$$

It should be noted that in eqs 12 and 13, the longest mode of the Rouse relaxation process has a characteristic time equal to $\tau_R(2M_{\text{branch}})$, and not $\tau_R(M_{\text{branch}})$. This choice is motivated by two considerations which reflect the fact that there are two branches at a branch point; hence the associated span molar mass is $2M_{\text{branch}}$, which (i) ensures consistency with the Rouse time of an equivalent linear chain of mass $2M_{\text{branch}}$, and (ii) accounts for the reduced mobility of the branching point.[44] While determining the exact longest relaxation time of the Rouse relaxation would require solving the full Rouse model for comb architecture, it is found here and in ref 44 (where the solution of the exact Rouse modes for H polymers was presented) that this approximation leads to a good description of the longest relaxation time of the arms.

3.3. Backbone Relaxation. For most samples, the weight fraction of the backbone is very low (see Table 2) and the comb backbones are considered not entangled with other comb backbones. Indeed, after the relaxation of the linear matrix and the comb branches, the number of backbone−backbone entanglements per macromolecule is $Z_{\text{BB}} = 3.5$ (using dilution exponent α of 1), which corresponds to a marginally entangled state. Note that if we used α of 1.3,[53] we would end-up with $Z_{\text{BB}} = 1.5$. Hence, we can consider that the comb backbones relax by CRR processes. As mentioned in the Introduction, two different scenarios are possible:

(1) When the linear matrix relaxes faster than the comb branches, as illustrated in Figure 3a, the relaxation of the backbone by Rouse and CRR processes is divided in three steps: at short times, the molecular segments of molar mass lower than the average molar mass between two entanglements or branching points ($M_{e,xx}$) relax by intrinsic Rouse modes, where

$$M_{e,xx} = \left(\frac{1}{M_e} + \frac{1}{M_{xx}}\right)^{-1} \tag{14}$$

based on the classical rubber elasticity theory.[18] Then, the modes involving molecular segments longer than $M_{e,xx}$ but shorter than the molar mass between two branching point, M_{xx}, relax at the rhythm of the release and (re)formation of entanglements with the linear matrix. Therefore, the delay of this CRR process compared to the intrinsic Rouse time is θ_{matrix}.

https://doi.org/10.1021/acs.macromol.1c01329
Macromolecules 2021, 54, 11047−11060

Finally, the longest modes are further delayed by a factor θ_{comb}, which takes into account the slow motions of the branching points, leading to extra friction coming from the branches. The delay θ_{comb} corresponds to the case where the comb branches are relaxing by the intrinsic Rouse process. However, because the relaxation of the latter ones is also delayed by a factor θ_{matrix} due to slow relaxation of the linear matrix, the CRR process of the backbone takes place with a total delay $\theta_{comb}\theta_{matrix}$, compared to its intrinsic Rouse relaxation. Thus, this approach accounts implicitly for the branch point hopping via the parameter $\theta_{comb}\theta_{matrix}$.

In this case, the corresponding relaxation function of the backbone is therefore described as[25,44]

$$G_{BB}(t) = \frac{\rho RT}{M_{BB}}\left(\sum_{p=1}^{p=q}\exp\left(\frac{-2p^2}{\theta_{comb}\theta_{matrix}\tau_R(M_{BB})}\right) + \sum_{p=q+1}^{p=Z_{e,xx}}\exp\left(\frac{-2p^2}{\theta_{matrix}\tau_R(M_{BB})}\right) + \sum_{p=Z_{e,xx}+1}^{p=N}\exp\left(\frac{-2p^2}{\tau_R(M_{BB})}\right)\right) \quad (15)$$

with $Z_{e,xx}$ being the number of entanglements or branching points along the backbone (see Figure 3) and q, the number of branches along the backbone. It should be noted that while the Rouse time of the backbone is determined by considering the entire backbone, the outer free ends of the backbone, which have a molar mass of 29 kg/mol, are considered to relax with the branches.[10,11,13] This is taken into account in the way the weight fractions ν_{BB} and ν_{branch} have been defined (see Table 2).

(2) On the contrary, if the branches of the comb relax faster than the linear matrix, the intermediate relaxation modes of the backbone are active before the disentanglement of the linear matrix; therefore, they are delayed only due to the friction coming from the branches, $\theta_{comb\text{-}ent}$ (see Figure 3b). Then, at longer times, the influence of the branches on the slow relaxation of the backbone becomes negligible compared to the influence of the linear matrix. Neglecting their effect, the CRR time of the backbone is expected to be delayed by a factor θ_{matrix}. The corresponding modulus is therefore written as

$$G_{BB}(t) = \frac{\rho RT}{M_{BB}}\left(\sum_{p=1}^{p=Z_{BB\text{-}lin}}\exp\left(\frac{-2p^2}{\theta_{matrix}\tau_R(M_{BB})}\right) + \sum_{p=Z_{BB\text{-}lin}+1}^{p=Z_{e,xx}}\exp\left(\frac{-2p^2}{\theta_{comb\text{-}ent}\tau_R(M_{BB})}\right) + \sum_{p=Z_{e,xx}+1}^{p=N}\exp\left(\frac{-2p^2}{\tau_R(M_{BB})}\right)\right) \quad (16)$$

with $Z_{BB\text{-}lin} = (\nu_{BB} + \nu_{linear})Z_{BB}$ being the number of active strands along the backbone after the relaxation of the branches (see Figure 3b). In this specific case, the value of $\theta_{comb\text{-}ent}$ is different from θ_{comb} in eq 15 because the branches relax dominantly by retraction rather than by Rouse. Because their relaxation is slower, it is expected that $\theta_{comb\text{-}ent}$ is larger than θ_{comb}. As further discussed in Section 5.5 below, it is however difficult to experimentally extract $\theta_{comb\text{-}ent}$ because the intermediate relaxation modes have a negligible effect in the experimental relaxation time spectrum. Only the delay induced by the matrix on the slow relaxation modes of the backbone, θ_{matrix}, can be definitely obtained by fitting the terminal regime of the spectrum.

For large concentrations of the comb polymer, the presence of backbone−backbone entanglements is possible. In this case, the backbone relaxation by Rouse and CRR processes is possible only up to the time when the molecular segments between two backbone−backbone entanglements, $M_{e,BB}$, are relaxed. If we consider that the linear matrix relaxes faster than the branches and if $Z_{e,BB} = M_{BB}/M_{e,BB}$ represents the number of backbone−backbone entanglement segments, the relaxation modulus of the backbone is described by

$$G_{BB}(t) = G_{0,BB}\varphi_{BB}(t)^2 + \frac{\rho RT}{M_{BB}}\left(\sum_{p=Z_{e,BB}+1}^{p=q}\exp\left(\frac{-2p^2}{\theta_{comb}\theta_{matrix}\tau_R(M_{BB})}\right) + \sum_{p=q+1}^{p=Z_{e,xx}}\exp\left(\frac{-2p^2}{\theta_{matrix}\tau_R(M_{BB})}\right) + \sum_{p=Z_{e,xx}+1}^{p=N}\exp\left(\frac{-2p^2}{\tau_R(M_{BB})}\right)\right) \quad (17)$$

In this eq 17, $G_{0,BB} = 4\rho\nu_{BB}RT/5M_{e,BB}$ is the low-frequency plateau modulus due to backbone−backbone entanglements, and the function $\varphi_{BB}(t)$ represents the survival fraction of initial backbone−backbone entanglement segments at time t.[54] Its exact definition is discussed in Section 5.6.

The different equations proposed in this section are tested and compared to the experimental data in Section 5.

4. LVE OF COMB/LINEAR BLEND

The LVE of the comb polymer C742 has been carefully investigated in the past.[11,47] Here, we use the data from ref 47. Figure 4a−c depicts the LVE master curves of the dynamic storage and loss moduli G' and G'' for all pure polymers and comb/linear blends as a function of angular frequency ω at a reference temperature T_{ref}, which is discussed below. The time−temperature superposition principle was employed to construct the master curves.[57] The data were first shifted vertically with a factor $b_T = [\rho(T_{ref}) \times (T_{ref} + 273.2)]/\rho(T) \times (T + 273.2)]$, with T being the temperature in °C and ρ being the density in g/cm^3, which depends on temperature as $\rho(T) = 1.2503 - 6.05 \times 10^{-4}(273.2 + T)$.[58] Subsequently, the data were shifted along the frequency axis. The horizontal shift factors a_T overlap for all samples and are fitted with the empirical WLF equation:[57] $\log(a_T) = [-C_1(T - T_{ref})]/[C_2 + T - T_{ref}]$, with $C_1 = 6.10$ and $C_2 = 110$ °C. A value of $T_g = 106$ °C was chosen as the reference transition temperature, $T_{g,ref}$. Because differences of T_g correspond to the horizontal shift along the frequency axis, the data for samples PS5k, PS64k, and PS1M must be plotted at iso-T_g conditions,[59] that is, $(T_{ref} - T_g) = 54$ °C. Therefore, the reference temperatures used for samples PS5k, PS64k, and PS1M are 141.6, 158, and 161 °C, respectively. Concerning the blends, their T_g values are estimated by means of the Fox equation $1/T_{g,blend} = \nu/T_{g,1} + (1 - \nu)/T_{g,2}$, where 1 and 2 refer to the two constituents of the blend and ν is the volume fraction.[60,61] $T_{g,blend}$s are equal to 90.6, 104, and 107 °C for

https://doi.org/10.1021/acs.macromol.1c01329
Macromolecules 2021, 54, 11047−11060

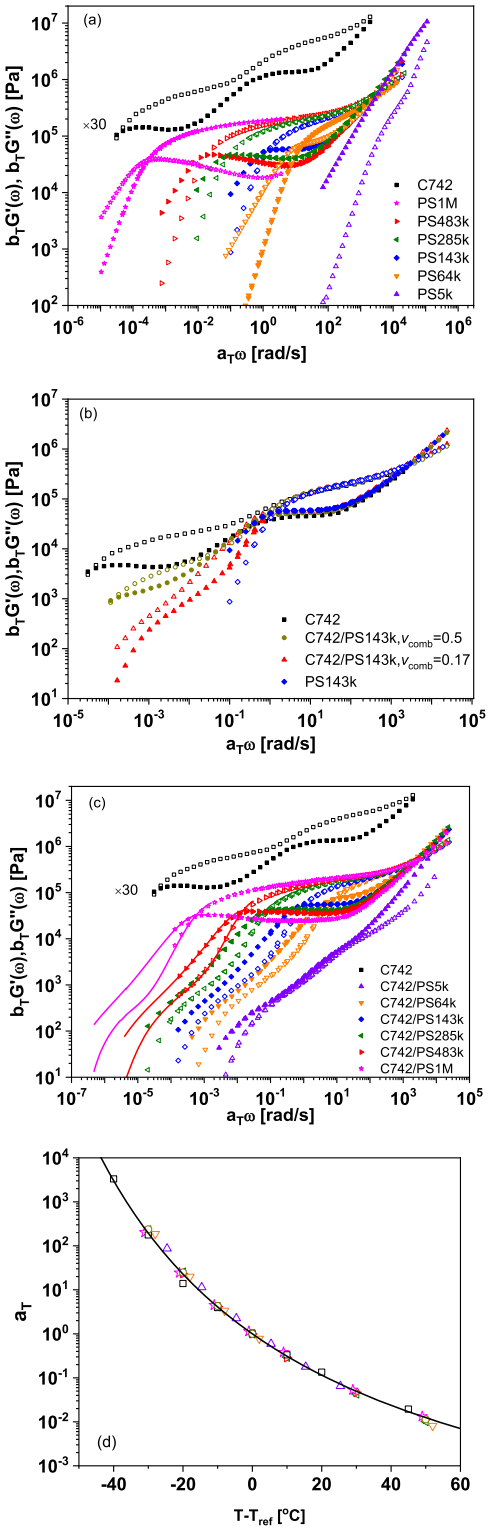

Figure 4. Shifted storage (open) and loss (closed) moduli under iso-T_g conditions, with $(T_{ref} - T_g) = 54$ °C, as a function of the shifted angular frequency for (a) C742 and linear chains, (b) C742/PS143k blends with $\nu_{comb} = 1$, 0.5, 0.17, and 0, and (c) C742/PSXk blends with $\nu_{comb} = 0.17$. The curves in (c) were transformed from creep data. Data of C742 in (a,c) were vertically shifted by factors of 30 for clarity. (d) Horizontal shift factor, a_T, as a function of $T - T_{ref}$ for all blends. The solid curve is the WLF fit with $C_1 = 6.10$ and $C_2 = 110$ °C. The symbols are the same as (c).

C742/PS5k, C742/PS64k, and C742/PS1M, respectively. Therefore, their reference temperatures are equal to 144.6, 158, and 161 °C, respectively. The horizontal shift factors are shown in Figure 4d.

The LVE data are presented in three groups: one including the pure melts (Figure 4a), one including C742 and its blends with PS143k at two different concentrations (Figure 4b), and one including C742 and its blends with the different M_w linear chains at the same concentration (Figure 4c). Figure 4a shows the moduli collapse at high frequencies, as expected due to virtually identical segmental and transitional Rouse-like motions. This confirms the reliability of the data and the fact that they are under iso-T_g conditions.[59] At lower frequencies, one can discern the rubbery plateau of the linear polymers and the additional slower relaxation peak (and associated lower plateau modulus) for the monodisperse comb polymer, which reflects the contribution of the diluted backbones.[11,13] Upon the addition of linear chains to the comb polymer, the level of this lower plateau decreases and the corresponding relaxation time is becoming shorter, as illustrated in Figure 4b with linear chains of 143 kg/mol at a volume fraction ν_{comb} of 1, 0.5, or 0.17, conforming to the dynamic dilution due to linear chains and from branches. For the more diluted blend ($\nu_{comb} = 0.17$), the low-ω plateau disappears and one can observe a power-law behavior $G', G'' \propto \omega^n$, with n being 1/2, reflecting the CRR relaxation of the not-self-entangled backbone, as observed before with other H-[9,15,44] and comb[11−14] polymers and further discussed in Section 3.

Several LVE parameters were extracted from the master curves and collected in Table 3. The zero-shear viscosity η_0 and recoverable compliance J_e^0 were obtained and averaged by three methods: taking the point at the lowest frequency, fitting the available dynamic complex viscosity data by means of the Cross model, and fitting by means of the Carreau model. The terminal relaxation time was calculated as $\tau_{BB} = \eta_0 J_e^0$ and is shown in Figure 5 as a function of the molar mass of the linear matrix. In most blends, the relaxation times of the linear chains and the comb branches cannot be distinguished, as discussed in Section 5, with the help of our model. A specific relaxation time that can be extracted is the reciprocal of the $G' - G''$ crossover frequency, $\tau_{c,blend}$, which appears after the high-frequency entanglement plateau. This time reflects the relaxation of the linear matrix in the presence of the comb polymer. As shown in Figure 5, it is very similar to the relaxation time of the pure linear chains, $\tau_{c,linear}$ (see Table 1). This indicates that the relaxation of the linear component is not substantially affected by the presence of the comb.

In Figure 5, we also observe that τ_{BB} follows a similar—albeit not identical—trend compared to the relaxation time of the linear matrix, $\tau_{c,linear}$. As the molar mass of the linear matrix decreases, the times further deviate from each other. This will be further discussed in Section 5 in the context of the lifetime of an entanglement segment, τ_{obs}.

5. DISCUSSION

In this section, the experimental data of the monodisperse pure components and their blends are analyzed based on the model proposed in Section 3. In addition to the three material parameters, G_N^0, M_e, and τ_e, which are fixed based on our previous works,[44] the model requires determining the retardation factors θ_{comb} and θ_{matrix}. To this end, once the model is validated for the monodisperse linear matrices (see Section 5.1), we analyze the rheological data of the comb

https://doi.org/10.1021/acs.macromol.1c01329
Macromolecules 2021, 54, 11047−11060

Table 3. LVE Parameters of the Investigated Polymers and Blends at $(T - T_{ref}) = 54$ °C

	ν_{comb}	$\eta_0\ 10^{-5}$ (Pa·s)	$J_e^0\ 10^5$ (Pa^{-1})	τ_{BB} (s)	$\tau_{c,blend}$ (s)
C742	1.0	$(20 \pm 5) \times 10^2$	17 ± 7	$(32 \pm 6) \times 10^3$	
C742/PS5k	0.17	0.034 ± 0.001	$(19 \pm 1) \times 10$	6.6 ± 0.2	
C742/PS64k	0.17	1.4 ± 0.1	$(18 \pm 2) \times 10$	$(25 \pm 3) \times 10$	0.10
C742/PS143k	0.17	6.5 ± 0.1	$(22 \pm 2) \times 10$	$(15 \pm 2) \times 10^2$	1.1
C742/PS143k	0.50	$(21 \pm 2) \times 10$	38 ± 2	$(80 \pm 4) \times 10^2$	1.7
C742/PS285k	0.17	70 ± 7	93 ± 5	$(65 \pm 7) \times 10^2$	13
C742/PS483k	0.17	$(20 \pm 1) \times 10$	$(12 \pm 1) \times 10$	$(25 \pm 1) \times 10^3$	68
C742/PS1M	0.17	$(35 \pm 2) \times 10^2$	73 ± 3	$(25 \pm 1) \times 10^4$	2.1×10^3

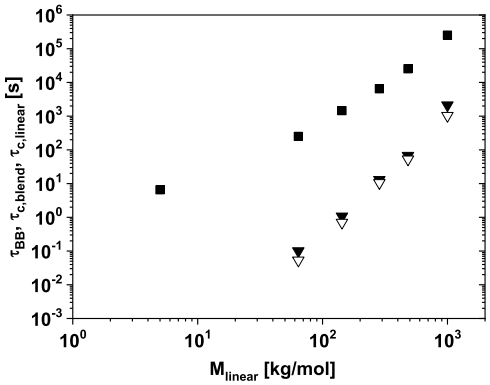

Figure 5. Backbone relaxation time τ_{BB} (■), the crossover relaxation time of blends $\tau_{c,blend}$ (▼), and the crossover relaxation time of pure linear chains $\tau_{c,linear}$ (▽) as a function of molar mass of linear components, M_{linear}. The comb composition in blends is 0.17.

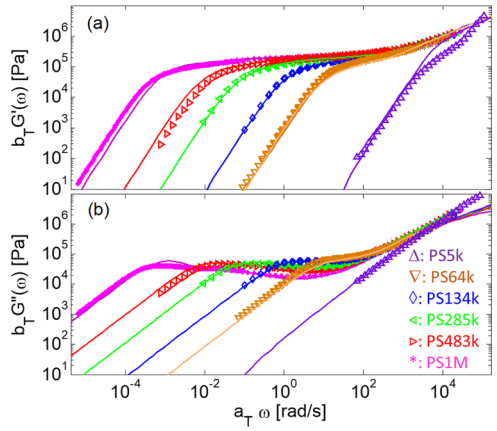

Figure 6. Comparison between the experimental (symbols) and the theoretical (−) storage (a) and loss (b) moduli for the linear matrices at $(T_{ref} - T_g) = 54$ °C.

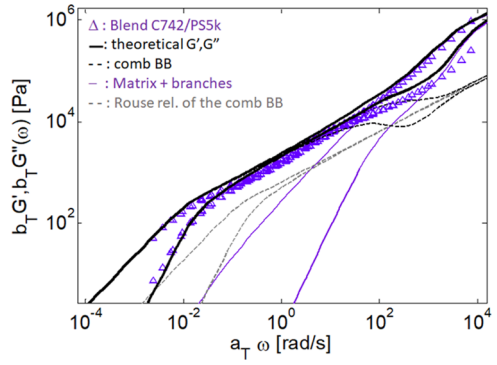

Figure 7. Comparison between the experimental (symbols) and the theoretical (black −) storage and loss moduli of the blend C742/PS5k at $(T - T_g) = 54$ °C. The contribution from the linear matrix and the branches is shown by the thin continuous curves. The Rouse relaxation and CRR relaxation of the backbone are shown by the gray and black dashed curves, respectively.

polymer diluted in an oligomeric matrix, for which it is expected that $\theta_{matrix} = 1$ (see Section 5.2). In this way, the delay factor for the Rouse relaxation of the backbone can be fully attributed to the friction coming from the branches, and the value of the constant θ_{comb} can be determined. The viscoelastic properties of the comb diluted in a short or in a long linear matrix are then analyzed in Sections 5.3 and 5.4, and the values determined by the best fitting procedure for the retardation factor θ_{matrix} are rationalized and discussed in Section 5.5. In Sections 5.6 and 5.7, the samples with the self-entangled backbone of the comb and pure combs are discussed, respectively.

5.1. LVE Properties of the Linear Matrices. We first apply our tube-based model (eqs 4−11) to predict the relaxation moduli of the linear matrix. The material parameters G_N^0, M_e, and τ_e have been set as 0.23 MPa, 14.8 kg/mol, and 2.3×10^{-3} s, respectively, at $(T_{ref} - T_g) = 54$ °C. Results are shown in Figure 6, along with the experimental data. It is evident that the model correctly predicts the relaxation of the linear matrix and can therefore be used as a starting point to model the LVE behavior of the blends.

5.2. Comb Polymer in an Oligomeric Matrix. The storage and loss moduli of the blend C742/PS5k are shown in Figure 7. Because the matrix is composed of oligomers, it relaxes by Rouse (see eq 5) at very high frequencies with $\tau_R(M_{matrix}) = 2.6 \times 10^{-4}$ s and does not contribute to the possible entanglements. Therefore, the molar mass between two entanglements must be rescaled as $M_{e,comb} = M_e/\nu_{comb} = 89$ kg/mol. This value is much larger than the molar mass of the branches (of 47 kg/mol), which therefore relax by a Rouse process (see eq 13). The relaxation of both the linear matrix and the branches is shown in Figure 7. On the other hand, the comb backbone can only relax after the relaxation of its branches. Because it represents only 6% of the sample (see Table 2), it contains virtually no effective backbone−backbone entanglements and its relaxation is described by a Rouse process, with typical slopes a 1/2 observed for G' and G''. As discussed in Section 3, this Rouse process must be delayed due to the extra friction arising from the slow motions of the branching points. This is also observed in Figure 7, where the intrinsic Rouse relaxation of the backbone is represented by the dashed gray curves. While these curves correctly capture the shape of the experimental data, they underpredict the relaxation spectrum (shifted to high frequencies compared to the data).

Therefore, we consider that the comb backbones relax by CRR (see eq 15), with no delay coming from the matrix ($\theta_{matrix} = 1$), but with a retardation factor due to the friction from the

https://doi.org/10.1021/acs.macromol.1c01329
Macromolecules 2021, 54, 11047−11060

branches, θ_{comb}. This parameter is determined by the best-fit procedure and its value is set as $\theta_{comb} = 12$. Because this value should not depend on the molar mass of the linear matrix in case the branches relax slower than linear chains ($\tau_{branch} > \tau_{linear}$), it is used for all these blends analyzed in the Section 5.3.

Thus, in the Rouse motion, the dynamics of arm and backbone are coupled until the relaxing subsection of the backbone has expanded to M_{xx}, the strand between branching points. From this point on, the Rouse motion of the backbone begins to feel the delay of the branching point (or the "fixed" branching points), as reflected by the retardation factor θ_{comb}. This mechanism is possible in this comb because the molar mass of the branch M_{branch} (47 kg/mol) is larger than M_{xx} (29 kg/mol), hence completing its Rouse or CRR relaxation slower. The delay coming from branching points results in a relatively large θ_{comb} value (= 12). In contrast, the delay factor for H-polymers, θ_H, is only 1.7,[44] indicating the low sensitivity of backbone Rouse relaxation to the branching points (*i.e.*, the branching points are not "fixed"). This is probably because the arms in H-polymers have almost the same molar mass as M_{xx} of the inner backbone, say, $M_{branch} = M_{xx}$. However, more work will be needed to elucidate this point in the future. In particular, we cannot exclude a slight overestimation of the value of θ_{comb} due to the presence of a few backbone−backbone entanglements. Figure 7 evidently illustrates the importance of the retardation effect coming from branching points. Without considering the retardation (setting $\theta_{comb} = 1$), the theoretical fitting significantly underestimates both the Rouse relaxation of the backbone and its terminal relaxation time.

5.3. Comb Polymer in a Short Chain Matrix ($\tau_{branch} > \tau_{linear}$). If the linear matrix PS64k is used to dilute the comb polymer, it is ensured that the linear matrix relaxes before the branches of the comb. Because the branches are entangled with the polymer matrix and because their relaxation time is not expected to be largely different (see Figure 4), we consider that both the linear chains and the comb branches relax by reptation and CLF, as described by our tube model (see eqs 4−11). Thus, the branches relax similarly to a linear polymer, from $x = 0$ at the extremity to $x = 1$ at the branching point, with imposing the restriction that reptation is not possible. During the relaxation of the linear chains and the branches, the fraction of the (inner) backbone relaxed is considered as equal to 0.

The relaxation of both the linear chains and the branches in sample C742/PS143k can be modeled in the same way as with PS64k. In this case, these two components have the same relaxation times.

Because for these two samples, the linear matrix is entangled with the comb backbone, and the latter will partially relax by the CRR process governed by the disentanglement/re-entanglement of the matrix, as illustrated in Figure 3a. This CRR process, which takes place with a retardation factor θ_{matrix} compared to the intrinsic Rouse process, stops when it reaches the relaxation time of the molecular segments of mass $M_{xx} = 28.6$ kg/mol, corresponding to the molar mass of the segments between two branching points. At this stage, longer Rouse modes involve the motion of the branching points, hence an extra delay which has been defined as $\theta_{comb} = 12$. The relaxation of the backbone is therefore well described by eq 15, as confirmed in Figure 8, which compares the theoretical and the experimental viscoelastic data of the blends. In order to correctly describe the data, the retardation factor θ_{matrix} has been fixed to 6.7 and 29.2 for the linear matrix PS64k and PS143k, respectively.

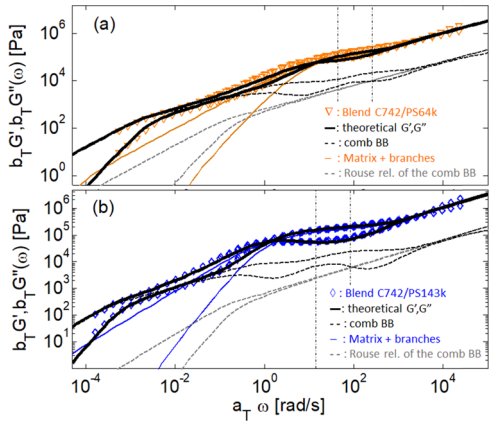

Figure 8. Comparison between the experimental (symbols) and the theoretical (black curves) storage and loss moduli of the blends C742/PS64k (a) and C742/PS143k (b) at $(T - T_g) = 54$ °C. The contribution from the linear matrix and the branches is shown by the thin continuous curves. The Rouse relaxation and CRR relaxation of the backbone are shown by the thin and thick dashed gray curves, respectively. The regime between the vertical dashed-dotted lines corresponds to the intermediate CRR relaxation of backbones from $M_{e,xx}$ to M_{xx}.

In Figure 8, the contributions of the different components to the storage and loss moduli can be observed. In particular, we see that terminal CRR relaxation of the backbone (from M_{xx} to M_{BB}) starts approximately at the crossover frequency, that is, the relaxation time of the linear chains (see Figure 5). However, the intermediate CRR relaxation (from $M_{e,xx}$ to M_{xx}), which only requires the motion of the matrix, starts much before the relaxation time of the latter, in agreement with the results found previously[44] and eqs 2 and 3. This will be further discussed in Section 5.5, based on the analysis of θ_{matrix}. We also observe that the intermediate regime (between the vertical dashed-dotted lines) is rather short, which is easily explained because it only concerns the relaxation of the molecular segments from $M_{e,xx} = 9.7$ kg/mol to $M_{xx} = 28.6$ kg/mol, while the molar mass of the entire backbone is of 860 kg/mol. The negligible influence of the intermediate matrix-dominated CRR process also suggests that other values of θ_{matrix} and θ_{comb} could have been used to describe the data, as long as their product $\theta_{matrix}\theta_{comb}$ is kept constant. However, because θ_{comb} has been fixed in Section 5.1, θ_{matrix} can be fixed without this degree of freedom. Nevertheless, it is important to discuss the validity of the chosen values, as proposed in Section 5.5.

5.4. Comb Polymer in a Long Chain Matrix ($\tau_{branch} < \tau_{linear}$). For the blends for which of the branch's relaxation time $\tau_{branch} < \tau_{c,linear}$ (*e.g.*, PS285k, PS483k, and PS1M), first, the branches relax, enhancing the mobility of the backbone, which can explore a dilated tube formed only by the entanglements with the linear chains. This is described by a CRR process at the rhythm of the disentanglement and re-entanglement of the branches, allowing for the relaxation of backbone segments having mass between $M_{e,xx}$ and $M_e/(\nu_{BB} + \nu_{linear})$. Subsequently, as observed in Figure 3b, the relaxation of the linear matrix takes place, followed by the relaxation of the backbone. It is important to note here the fact that the relaxation time of the backbone in the monodisperse comb is similar to the relaxation time of the linear matrix does not imply that the comb backbone will relax in a thin and undiluted tube. Indeed, the relaxation by reptation or CLF of the backbone of a comb blended with very long linear chains is expected to be much slower than the respective

https://doi.org/10.1021/acs.macromol.1c01329
Macromolecules 2021, 54, 11047−11060

relaxation time in the pure comb melt; the reason is that in the blends, the branches represent only a small fraction of the sample, and hence, the DTD process is much weaker in the case of a long linear matrix, which slows down the relaxation of the backbone in comparison to the pure comb. In fact, the terminal relaxation process of the backbone is well described by a CRR process governed by the matrix alone, as the influence of the branches becomes negligible (see eq 16). This equation is shown in Figure 9. As the value of $\theta_{comb\text{-}ent}$ is not known, we fix it

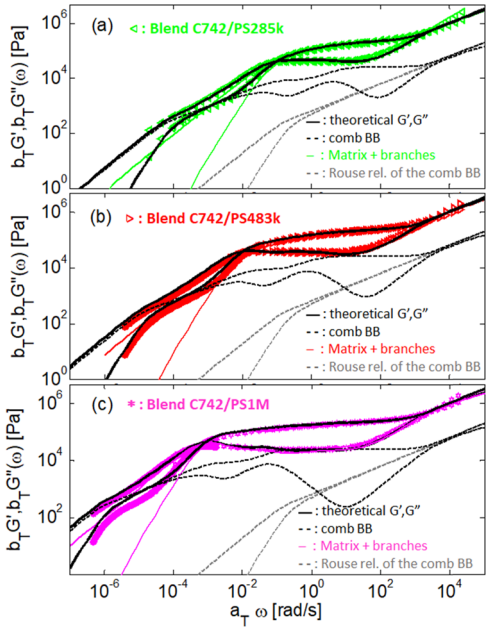

Figure 9. Comparison between the experimental (symbols) and the theoretical (black curves) storage and loss moduli of the blends C742/PS285k (a), C742/PS483k (b), and C742/PS1M (c) at $(T - T_g) = 54$ °C. The contribution from the linear matrix and the branches is shown by the thin continuous curves. The Rouse relaxation and CRR relaxation of the backbone are shown by the thin and thick dashed gray curves, respectively.

here as equal to θ_{comb}. As already mentioned, because the relaxation of the entangled branches is slower than the Rouse relaxation of the backbone, the latter value is underestimated. However, its influence on the data is negligible.

A good agreement is found by using a delay factor θ_{matrix} = 2500, 12,500, and 180,000 for the linear matrix of mass 285, 483, and 1000 kg/mol, respectively, on the backbone Rouse relaxation, compared to its intrinsic Rouse process. We note however a slight deviation at low frequencies, with the predictions slightly overestimating the terminal relaxation of the comb. This could be due to the possible relaxation of the inner backbone extremities (after the relaxation of branches and the free ends of backbones) by CLF before the CRR takes place.[11,13] The fitting result cannot be further improved by tuning the values of θ_{matrix}. The issue here is that whatever the value of θ_{matrix} is, the predicted relaxation shoulder in G' is too high compared to the experimental one. Therefore, we have fixed the value of θ_{matrix}, which has been determined by the best fitting procedure, in order to ensure keeping the right shape of this shoulder, despite the shift observed. The resulting fitting of the whole spectrum was satisfactory.

5.5. Retardation Factors of the Comb Polymer in Linear Matrices. In Figure 10, the values of θ_{matrix} are plotted as

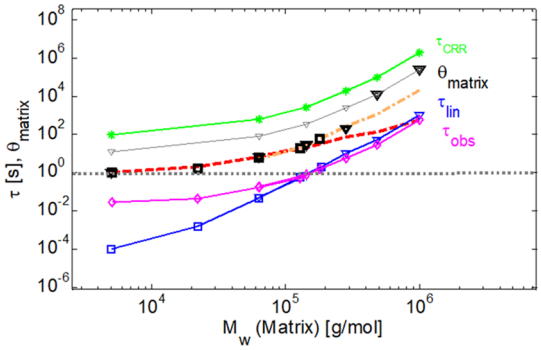

Figure 10. Extracted values of the matrix retardation factor θ_{matrix} (black symbols) *vs* the molar mass of the linear matrix for the comb/linear blends (black ∇) or for the H/linear blends[44] (□), and relaxation time of the linear matrix (blue), eqs 2 (orange dashed-dotted) and 3 (red dashed). The values of the overall delay θ_{tot} on the Rouse relaxation time of the backbone, with $\theta_{tot} = \theta_{matrix}\theta_{comb}$ if $(\tau_{branch} > \tau_{linear})$ and $\theta_{tot} = \theta_{matrix}$ if $(\tau_{branch} < \tau_{linear})$, are also presented (gray ∇), as well as the value of τ_{obs}, equal to $\theta_{tot}\tau_e$ (magenta ◊), and the CRR time of the backbone (green*).

a function of the molar mass of the linear matrix. These data are compared to the crossover relaxation time of the linear polymers and the scaling proposed in eq 2 (orange dashed-dotted curve) and eq 3 (red dashed curve). The values of the overall delay θ_{tot} on the Rouse relaxation time of the backbone, with $\theta_{tot} = \theta_{matrix}\theta_{comb}$ if $(\tau_{branch} > \tau_{linear})$ and $\theta_{tot} = \theta_{matrix}$ if $(\tau_{branch} < \tau_{linear})$, are also shown (gray ∇), as well as that on the CRR time of the backbone, equal to $\theta_{tot}\tau_R(M_{BB})$ (green curve).

First, one may remark that at high molar mass of the linear matrix, both the retardation factor θ_{tot} (or equivalently, the CRR time) and the relaxation time of the linear chains follow the same trend, as predicted by the Graessley−Struglinski relationship,[26] $\tau_{CRR} = \tau_{obs}Z_{BB}^2$, with τ_{obs} representing the average lifetime of an entanglement segment. According to the Graessley−Struglinski criterion, $\tau_{obs} = \tau_{linear}$, which can be compared to the value determined from the experimental data and is equal to the ratio $\tau_{CRR}/Z_{BB}^2 = \theta_{tot}\tau_e$. As seen in Figure 10, τ_{obs} is indeed very similar to τ_{linear} for the larger molar mass matrices, which corresponds to the case for which the matrix relaxes similarly or slower than the comb branches. Therefore, we can conclude that in this regime: (i) the Graessley−Struglinski criterion for linear−linear blends[26] is valid, (ii) the CRR relaxation of the comb backbone is strongly dominated by the linear matrix, and (iii) the influence of the extra friction coming from the branching points is negligible, which is in good agreement with the assumption made in eq 16 according to which the delay on the Rouse relaxation of the backbone is only due to the long linear matrix. From the values of θ_{matrix}, we can remark that in this regime, both eqs 2 and 3 underestimate the influence of the matrix. However, the key assumption that the fast motions of the branches do not significantly affect the long Rouse relaxation modes of the comb backbones should be further tested. Because this cannot be done based on binary blends of linear chains (as it requires very long "short chains"), one should test it on another comb polymer. It must also be noted that in the case of the comb/PS285k blends, the value of θ_{matrix} is probably slightly underestimated due to the fact that we consider that the backbone relaxation is fully dominated by the branch motion, ignoring the possible disentanglement of the backbone extremities, taking place in a thin tube, and which in reality should also play a role. On the other hand, in the regime in which the linear matrix is relaxing

https://doi.org/10.1021/acs.macromol.1c01329
Macromolecules 2021, 54, 11047−11060

faster than the comb branches, the Graessley−Struglinski criterion strongly deviates, in agreement with findings of previous works.[44]

The retardation factors of the comb/linear blends are also compared to the retardation factors found in our previous work for H/linear blends.[44] A very good overlap between the curves is found. This result suggests that the retardation factor governed by the slow motion of the matrix, which delays the relaxation of the entire comb, does not depend on the molecular structure (architecture) of the comb but only on the matrix instead. More importantly, it suggests that as long as the relaxation of the backbone of a complex architecture is mostly governed by the motion of its branches, we may decouple the retardation effect coming from the matrix, θ_{matrix}, and the retardation factor coming from the branches of the complex architecture, θ_{comb} = 12 and θ_H = 1.7 (for H-polymers), which provides a new tool to control the relaxation and viscosity of such complex polymeric blends. As a perspective, in order to obtain a fully predictive model, one should understand how the retardation factor associated to the complex macromolecules depends on its architecture. Obviously, this parameter should depend on the number and molar mass of the branches attached to the backbone. However, more experimental data are needed in order to fully understand their effects.

5.6. Comb/Linear Blends at Large Concentrations: Self-Entangled Backbones. As mentioned in Section 3, if the concentration of the comb polymer is increased, the backbones of the combs are also entangled with other backbones and the CRR process does not lead to the full relaxation of the sample. In this section, the viscoelastic behavior of the blend composed of 50% of C742 and 50% of PS143k is analyzed with the objective to assess whether the retardation factors determined in the diluted regime can also be used in this case. Once the linear matrix and branches of the combs relax, the molar mass between two backbone−backbone entanglements can be estimated as $M_{e,BB}$ = 82 kg/mol, that is, the backbone contains around 10 entanglements with other backbones.

To this end, we first model the two extreme situations, that is, either assuming that the backbone relaxes up to the level of the backbone−backbone entanglements, which are considered as permanent (*i.e.,* considering eq 17 with $\varphi = 1$) or assuming that it fully relaxes by CRR (*i.e.,* considering eq 15), without any effect of these entanglements. While the latter assumption is certainly not correct, it allows for highlighting the effect of the entanglements. Results are shown in Figure 11a. The predicted curves have been obtained by using the retardation factors found in Section 5.2 for the comb diluted in PS143k. It is seen that considering that the CRR process stops at the level of $M_{e,BB}$ correctly describes the experimental data at high frequencies. Moreover, the influence of backbone−backbone entanglements is also clearly observed by looking at the discrepancy between the experimental data and the data predicted by assuming the full CRR process.

After the relaxation of the linear matrix and of the branches, the relaxation of the entangled backbones follows. It takes place in a diluted tube by reptation and is influenced (here, dominated) by the preceding branch point hopping mechanism.[9,12] The dilution state of the tube corresponds to the tube formed only by the backbone−backbone entanglements, that is, considering that only a fraction ν_{BB} of the sample is not relaxed. To describe it, we first rescale the material parameters accordingly (see eq 17)[37,38]

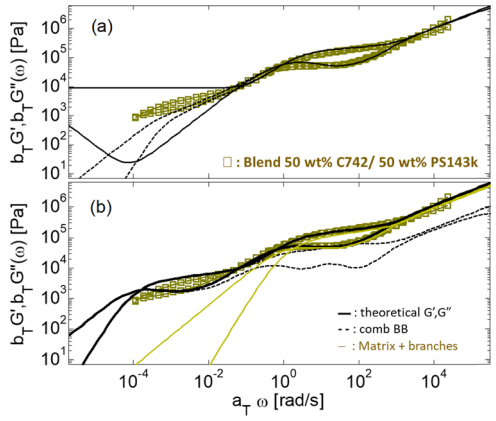

Figure 11. Comparison between the experimental (symbols) and theoretical (curves) storage and loss moduli of the blend composed of 50% of C742 and 50% of PS143k at T = 160 °C. (a) Predicted curves determined by assuming that the backbone−backbone entanglement segments do not relax (−) or by assuming full CRR (--); (b) Predicted data determined by assuming that the backbones are self-entangled and relax according to eq 22 (−). The dashed curve shows the contribution from the comb backbones and the thin continuous curve and the contribution from the linear matrix and the comb branches.

$$M_{e,BB} = \frac{M_e}{\nu_{BB}} \tag{18}$$

$$G_{0,BB} = G_N^0 \nu_{BB}^2 \tag{19}$$

$$\tau_{e,BB} = \frac{\tau_e}{\nu_{BB}^2} \tag{20}$$

with ν_{BB} = 18% (see Table 2). Because each entanglement segment $M_{e,BB}$ contains several branch points, we then account for the retardation effect induced by the slow motion of the branch points by considering a delay factor on the relaxation time of an entanglement segment, $\tau_{e,BB}$. To this end, the intrinsic Rouse time of a backbone−backbone entanglement segment, $\tau_{e,BB}$, is replaced by its corresponding CRR time

$$\tau_{e,BB,CRR} = \theta_{matrix}\theta_{comb}\tau_{e,BB} \tag{21}$$

In the latter expression, it is assumed that the relaxation of a backbone−backbone entanglement segment is a Rouse process governed by the motion of the branch points it contains, while the relaxation of the branches is delayed by the linear matrix (see also discussion on pure comb melts below).

This new parameter is used along with $M_{e,BB}$ and $G_{0,BB}$ in our tube model to determine the survival probability of the entanglement segments. At this level, the backbones are thus considered as linear chains bearing extra friction, which is taken into account in the value of $\tau_{e,BB,CRR}$. Their reptation times are therefore equal to[38−40]

$$\tau_{rept} = 3\tau_{e,BB,CRR}\left(\frac{\frac{28}{30}M_{BB}}{M_{e,BB}}\right)^3 \tag{22}$$

It must be noted here that only the inner backbone has been considered to determine the reptation time because the relaxation of the outer segments is much faster than the relaxation of the inner part.[11] Considering the whole backbone would have led to a reptation time 1.2 times slower.[15]

https://doi.org/10.1021/acs.macromol.1c01329
Macromolecules 2021, 54, 11047−11060

As shown in Figure 11b, using this molecular picture provides a satisfactory description of the terminal relaxation of the comb backbones (see the dashed curves in the figure). Addition of the CRR modes, which take places until the backbone−backbone entanglement segments are relaxed (see eq 17), leads to a good prediction of the entire viscoelastic spectrum. Therefore, this result suggests that our model based on the retardation factors can be extended to entangled systems, as long as the hierarchical nature of the relaxation of the branches and the backbone is preserved and as long as the density of branch points is larger than the density of backbone−backbone entanglements.

As a last comment, it must be noted that the dilution exponent α has been fixed to 1 in eqs 20−22. This is justified as the model accounts for the early fluctuations of the backbone in its dilated tube[36−38] and considers the outer backbone segments as the solvent. We see however that the predicted low frequency plateau is too pronounced and slightly overestimated, suggesting a too strong influence of the entanglements.

5.7. Pure Comb Melts. Given that the physics of comb polymer relaxation[10,11,13] is invoked in the presented analysis (and implicitly accounted for, along with CR effects, with the different delay factors), it is interesting to test the limiting case of our approach in the absence of the matrix polymer, that is, the case of monodisperse comb melt. In particular, we would like to see if the extra friction coming from the branch points can be included in the relaxation time of the backbone−backbone entanglement segments. We consider that the branches relax by fluctuations, after the high-frequency Rouse relaxation of the entanglement segments with molar mass M_e, and therefore, their contribution to the relaxation modulus is taken into account in eq 4. On the other hand, the backbone relaxes first by Rouse relaxation of its segments $M_{e,xx}$, and then, it relaxes by CRR induced by the relaxation of the branches. This CRR process takes place until the backbone segments of mass $M_{e,BB} = M_e/\nu_{BB}$ (with $\nu_{BB} = 0.36$) have relaxed. The CRR relaxation of the latter segments, $\tau_{e,BB,CRR}$, necessitates to account for the effects of both the $M_{e,BB}/M_e$ entanglements and the $M_{e,BB}/M_{xx}$ branch points. Because the lifetimes of these two groups of species are well approximated by the relaxation time of the branches, τ_{branch}, we can approximate the characteristic time of a backbone−backbone entanglement segment as $\tau_{e,BB,CRR} = \tau_{branch}(M_{e,BB}/M_{e,xx})^2 = 17.7\ \tau_{branch}$ (see eq 14). Defining the lifetime of the branches as the inverse of their G', G'' cross-over frequency (see the red curve in Figure 12), $\tau_{branch} = 0.29s$, we find that $\tau_{e,BB,CRR} = 5.15s$. The CRR relaxation of the backbone is followed by its reptation in the dilated tube (see eqs 18−20), governed by the hopping of the branch points. As the influence of the latter is accounted for in the value of $\tau_{e,BB,CRR}$, eq 22 can be used to determine the corresponding reptation time of the backbone.

The predicted curves are compared to the experimental curves shown in Figure 12, and a satisfactory agreement is found, despite the simplicity of the model proposed (which contains implicitly and in approximate form the correct physics of comb relaxation). It seems therefore possible to interpret the relaxation of the complex branched architecture based on its decomposition into different hierarchical levels of complexity, each level accounting for the retardation effect from the relaxation of the faster component. This result points to the internal consistency of the present approach.

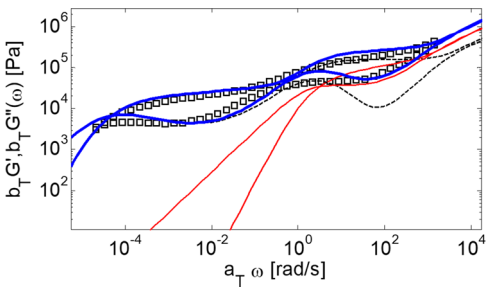

Figure 12. Comparison between the experimental (symbols) and the theoretical (thick continuous curves) storage and loss moduli of the monodisperse comb C742. The dashed curve shows the contribution from the comb backbones and the thin continuous curves and the contribution from the comb branches.

6. CONCLUDING REMARKS

This study addresses the LVE of topological blends involving a small fraction of monodisperse comb PSs in a matrix of linear PSs. Such a blend is dynamically a three-component system, comprising branches, backbones, and linear chains. We examine systematically the relaxation of the same diluted comb having relatively short arms (relaxing by Rouse modes) and even shorter segments between branches, as a function of the molar mass of the linear chain (oligomer, relaxation faster than or slower than that of the branches), as well as the case of backbone self-entanglements. We develop a model for the contributions of the three components to comb relaxation by accounting for the dynamic dilution and two delay factors, one due to the matrix and another due to the comb. The former represents the frictional contribution of the linear polymers to the constraint released Rouse process of the branches and backbone and the latter represents the relevant effect of the branches on the backbone. When the branches relax slower than the matrix, the Rouse motions of the backbone are governed by the motion of the branches, which themselves are governed by the motion of the matrix. On the other hand, when the branches relax faster than the matrix, their influence is negligible compared to the matrix, and the Rouse motions of the backbone are mainly governed by the matrix. The model provides an excellent quantitative description of the experimental data. In addition, the resulting retardation factors in the relaxation process of the combs as a function of the linear polymer molar mass extend our earlier investigations of blends involving H-polymers in linear matrices,[44] suggesting a universal relaxation behavior of architecturally complex (branched) polymers in linear matrices based on CR mechanisms and the ability to tailor the dynamics of such composites at wish. This analysis with the delay factors accounts implicitly for the physics of comb polymer relaxation (hierarchical relaxation and branch point hopping) through the delay factors, and in the limiting case of the absence of the linear matrix, it predicts satisfactorily the viscoelasticity of pure comb melt, and hence, it is internally consistent. There are still some challenges to address in the future, such as the validation of the value of θ_{comb} and the coupling of branch and backbone motion. Nevertheless, the present results could open new directions in the tunability of polymeric blends involving architecturally complex macromolecules and the consideration of dynamic dilution in such composite materials.

AUTHOR INFORMATION

Corresponding Author

Zhi-Chao Yan − *Shenzhen Key Laboratory of Polymer Science and Technology, Guangdong Research Center for Interfacial Engineering of Functional Materials, College of Materials*

https://doi.org/10.1021/acs.macromol.1c01329
Macromolecules 2021, 54, 11047−11060

Science and Engineering, Shenzhen University, Shenzhen 518055, China; Institute of Electronic Structure and Laser, FORTH, Heraklion 71110, Greece; orcid.org/0000-0002-1447-9986; Email: yanzhch@szu.edu.cn

Authors

Evelyne van Ruymbeke − *Bio and Soft Matter, Institute on Condensed Matter and Nano-science, Université Catholique de Louvain, Louvain-la-Neuve 1348, Belgium;* orcid.org/0000-0001-7633-0194

Dimitris Vlassopoulos − *Institute of Electronic Structure and Laser, FORTH, Heraklion 71110, Greece; Department of Materials Science & Technology, University of Crete, Heraklion 71003, Greece;* orcid.org/0000-0003-0866-1930

Complete contact information is available at: https://pubs.acs.org/10.1021/acs.macromol.1c01329

Notes

The authors declare no competing financial interest.

■ ACKNOWLEDGMENTS

This work was supported by the National Natural Science Foundation of China (grant no. 21803039), Guangdong Basic and Applied Basic Research Foundation (grant no. 2020A1515010326), and Pearl River Talents Plan of Guangdong Province (2017GC010659). We thank J. Roovers for generously providing the PS combs used in this work and F. Snijkers and R. H. Colby for helpful discussions.

■ REFERENCES

(1) Doi, M.; Edwards, S. F. *The Theory of Polymer Dynamics*; Clarendon Press: Oxford, U.K., 1986.
(2) de Gennes, P. G. Reptation of a Polymer Chain in Presence of Fixed Obstacles. *J. Chem. Phys.* **1971**, *55*, 572−579.
(3) Likhtman, A. E.; McLeish, T. C. B. Quantitative Theory for Linear Dynamics of Linear Entangled Polymers. *Macromolecules* **2002**, *35*, 6332−6343.
(4) van Ruymbeke, E.; Liu, C.-Y.; Bailly, C. Quantitative Tube Model Predictions for the Linear Viscoelasticity of Linear Polymers. *Rheol. Rev.* **2007**, 53−134.
(5) Milner, S. T.; McLeish, T. C. B. Reptation and Contour-Length Fluctuations in Melts of Linear Polymers. *Phys. Rev. Lett.* **1998**, *81*, 725−728.
(6) Shchetnikava, V.; Slot, J.; van Ruymbeke, E. Comparative Analysis of Different Tube Models for Linear Rheology of Monodisperse Linear Entangled Polymers. *Polymers* **2019**, *11*, 754.
(7) Rubinstein, M.; Colby, R. H. Self-Consistent Theory of Polydisperse Entangled Polymers: Linear Viscoelasticity of Binary Blends. *J. Chem. Phys.* **1988**, *89*, 5291−5306.
(8) Larson, R. G. Combinatorial Rheology of Branched Polymer Melts. *Macromolecules* **2001**, *34*, 4556−4571.
(9) McLeish, T. C. B.; Allgaier, J.; Bick, D. K.; Bishko, G.; Biswas, P.; Blackwell, R.; Blottière, B.; Clarke, N.; Gibbs, B.; Groves, D. J.; Hakiki, A.; Heenan, R. K.; Johnson, J. M.; Kant, R.; Read, D. J.; Young, R. N. Dynamics of Entangled H-Polymers: Theory, Rheology, and Neutron-Scattering. *Macromolecules* **1999**, *32*, 6734−6758.
(10) Daniels, D. R.; McLeish, T. C. B.; Crosby, B. J.; Young, R. N.; Fernyhough, C. M. Molecular Rheology of Comb Polymer Melts. 1. Linear Viscoelastic Response. *Macromolecules* **2001**, *34*, 7025−7033.
(11) Kapnistos, M.; Vlassopoulos, D.; Roovers, J.; Leal, L. G. Linear Rheology of Architecturally Complex Macromolecules: Comb Polymers with Linear Backbones. *Macromolecules* **2005**, *38*, 7852−7862.
(12) Das, C.; Inkson, N. J.; Read, D. J.; Kelmanson, M. A.; McLeish, T. C. B. Computational Linear Rheology of General Branch-on-Branch Polymers. *J. Rheol.* **2006**, *50*, 207−234.
(13) Ahmadi, M.; Bailly, C.; Keunings, R.; Nekoomanesh, M.; Arabi, H.; van Ruymbeke, E. Time Marching Algorithm for Predicting the Linear Rheology of Monodisperse Comb Polymer Melts. *Macromolecules* **2011**, *44*, 647−659.
(14) Ahmadi, M.; Pioge, S.; Fustin, C.-A.; Gohy, J.-F.; van Ruymbeke, E. Closer Insight in the Structure of Moderate to Densely Branched Comb Polymers by Combining Modeling and Linear Rheological Measurements. *Soft Matter* **2017**, *13*, 1063−1073.
(15) van Ruymbeke, E.; Bailly, C.; Keunings, R.; Vlassopoulos, D. A General Methodology to Predict the Linear Rheology of Branched Polymers. *Macromolecules* **2006**, *39*, 6248−6259.
(16) van Ruymbeke, E.; Muliawan, E. B.; Hatzikiriakos, S. G.; Watanabe, T.; Hirao, A.; Vlassopoulos, D. Viscoelasticity and Extensional Rheology of Model Cayley-Tree Polymers of Different Generations. *J. Rheol.* **2010**, *54*, 643−662.
(17) Matsumiya, Y.; Masubuchi, Y.; Inoue, T.; Urakawa, O.; Liu, C.-Y.; van Ruymbeke, E.; Watanabe, H. Dielectric and Viscoelastic Behavior of Star-Branched Polyisoprene: Two Coarse-Grained Length Scales in Dynamic Tube Dilation. *Macromolecules* **2014**, *47*, 7637−7652.
(18) Rubinstein, M.; Colby, R. H. *Polymer Physics*; Oxford University Press: New York, 2003.
(19) Milner, S. T.; McLeish, T. C. B.; Young, R. N.; Hakiki, A.; Johnson, J. M. Dynamic Dilution, Constraint-Release, and Star-Linear Blends. *Macromolecules* **1998**, *31*, 9345−9353.
(20) Struglinski, M. J.; Graessley, W. W.; Fetters, L. J. Effects of Polydispersity on the Linear Viscoelastic Properties of Entangled Polymers. 3. Experimental-Observations on Binary-Mixtures of Linear and Star Polybutadienes. *Macromolecules* **1988**, *21*, 783−789.
(21) Watanabe, H.; Yoshida, H.; Kotaka, T. Entanglement in Blends of Monodisperse Star and Linear Polystyrenes. 1. Dilute Blends. *Macromolecules* **1988**, *21*, 2175−2183.
(22) van Ruymbeke, E.; Coppola, S.; Balacca, L.; Righi, S.; Vlassopoulos, D. Decoding the Viscoelastic Response of Polydisperse Star/Linear Polymer Blends. *J. Rheol.* **2010**, *54*, 507−538.
(23) Lee, J. H.; Archer, L. A. Stress Relaxation of Star/Linear Polymer Blends. *Macromolecules* **2002**, *35*, 6687−6696.
(24) Shivokhin, M. E.; van Ruymbeke, E.; Bailly, C.; Kouloumasis, D.; Hadjichristidis, N.; Likhtman, A. E. Understanding Constraint Release in Star/Linear Polymer Blends. *Macromolecules* **2014**, *47*, 2451−2463.
(25) Ebrahimi, T.; Taghipour, H.; Griessl, D.; Mehrkhodavandi, P.; Hatzikiriakos, S. G.; van Ruymbeke, E. Binary Blends of Entangled Star and Linear Poly(hydroxybutyrate): Effect of Constraint Release and Dynamic Tube Dilation. *Macromolecules* **2017**, *50*, 2535−2546.
(26) Struglinski, M. J.; Graessley, W. W. Effects of Polydispersity on the Linear Viscoelastic Properties of Entangled Polymers. 1. Experimental-Observations for Binary-Mixtures of Linear Polybutadiene. *Macromolecules* **1985**, *18*, 2630−2643.
(27) Green, P. F.; Mills, P. J.; Palmstrøm, C. J.; Mayer, J. W.; Kramer, E. J. Limits of Reptation in Polymer Melts. *Phys. Rev. Lett.* **1984**, *53*, 2145−2148.
(28) Park, S. J.; Larson, R. G. Tube Dilation and Reptation in Binary Blends of Monodisperse Linear Polymers. *Macromolecules* **2003**, *37*, 597−604.
(29) Watanabe, H. Viscoelasticity and Dynamics of Entangled Polymers. *Prog. Polym. Sci.* **1999**, *24*, 1253−1403.
(30) Viovy, J. L.; Rubinstein, M.; Colby, R. H. Constraint Release in Polymer Melts - Tube Reorganization Versus Tube Dilation. *Macromolecules* **1991**, *24*, 3587−3596.
(31) Marrucci, G. Relaxation by Reptation and Tube Enlargement - a Model for Polydisperse Polymers. *J. Polym. Sci., Polym. Phys.* **1985**, *23*, 159−177.
(32) Watanabe, H.; Matsumiya, Y.; van Ruymbeke, E. Component Relaxation Times in Entangled Binary Blends of Linear Chains: Reptation/CLF along Partially or Fully Dilated Tube. *Macromolecules* **2013**, *46*, 9296−9312.

(33) Watanabe, H.; Ishida, S.; Matsumiya, Y.; Inoue, T. Test of Full and Partial Tube Dilation Pictures in Entangled Blends of Linear Polyisoprenes. *Macromolecules* **2004**, *37*, 6619−6631.
(34) Watanabe, H.; Ishida, S.; Matsumiya, Y.; Inoue, T. Viscoelastic and Dielectric Behavior of Entangled Blends of Linear Polyisoprenes Having Widely Separated Molecular Weights: Test of Tube Dilation Picture. *Macromolecules* **2004**, *37*, 1937−1951.
(35) Blottière, B.; McLeish, T. C. B.; Hakiki, A.; Young, R. N.; Milner, S. T. Rheology and Tube Model Theory of Bimodal Blends of Star Polymer Melts. *Macromolecules* **1998**, *31*, 9295−9304.
(36) van Ruymbeke, E.; Masubuchi, Y.; Watanabe, H. Effective Value of the Dynamic Dilution Exponent in Bidisperse Linear Polymers: from 1 to 4/3. *Macromolecules* **2012**, *45*, 2085−2098.
(37) van Ruymbeke, E.; Shchetnikava, V.; Matsumiya, Y.; Watanabe, H. Dynamic Dilution Effect in Binary Blends of Linear Polymers with Well-Separated Molecular Weights. *Macromolecules* **2014**, *47*, 7653−7665.
(38) Shahid, T.; Huang, Q.; Oosterlinck, F.; Clasen, C.; van Ruymbeke, E. Dynamic Dilution Exponent in Monodisperse Entangled Polymer Solutions. *Soft Matter* **2017**, *13*, 269−282.
(39) Read, D. J.; Jagannathan, K.; Sukumaran, S. K.; Auhl, D. A Full-Chain Constitutive Model for Bidisperse Blends of Linear Polymers. *J. Rheol.* **2012**, *56*, 823−873.
(40) Read, D. J.; Shivokhin, M. E.; Likhtman, A. E. Contour Length Fluctuations and Constraint Release in Entangled Polymers: Slip-Spring Simulations and Their Implications for Binary Blend Rheology. *J. Rheol.* **2018**, *62*, 1017−1036.
(41) Park, S. J.; Larson, R. G. Long-Chain Dynamics in Binary Blends of Monodisperse Linear Polymers. *J. Rheol.* **2006**, *50*, 21−39.
(42) Brochard-Wyart, F.; Ajdari, A.; Leibler, L.; Rubinstein, M.; Viovy, J. L. Dynamics of Stars and Linear Chains Dissolved in a Polymer Melt. *Macromolecules* **1994**, *27*, 803−808.
(43) Shahid, T.; Clasen, C.; Oosterlinck, F.; van Ruymbeke, E. Diluting Entangled Polymers Affects Transient Hardening but Not Their Steady Elongational Viscosity. *Macromolecules* **2019**, *52*, 2521−2530.
(44) Lentzakis, H.; Costanzo, S.; Vlassopoulos, D.; Colby, R. H.; Read, D. J.; Lee, H.; Chang, T.; van Ruymbeke, E. Constraint Release Mechanisms for H-Polymers Moving in Linear Matrices of Varying Molar Masses. *Macromolecules* **2019**, *52*, 3010−3028.
(45) Roovers, J. Synthesis and Dilute Solution Characterization of Comb Polystyrenes. *Polymer* **1979**, *20*, 843−849.
(46) Lentzakis, H.; Vlassopoulos, D.; Read, D. J.; Lee, H.; Chang, T.; Driva, P.; Hadjichristidis, N. Uniaxial Extensional Rheology of Well-Characterized Comb Polymers. *J. Rheol.* **2013**, *57*, 605−625.
(47) Roovers, J.; Graessley, W. W. Melt Rheology of Some Model Comb Polystyrenes. *Macromolecules* **1981**, *14*, 766−773.
(48) Roovers, J. Melt Rheology of H-Shaped Polystyrenes. *Macromolecules* **1984**, *17*, 1196−1200.
(49) Snijkers, F.; Vlassopoulos, D. Cone-Partitioned-Plate Geometry for the ARES Rheometer with Temperature Control. *J. Rheol.* **2011**, *55*, 1167−1186.
(50) Yan, Z.-C.; Costanzo, S.; Jeong, Y.; Chang, T.; Vlassopoulos, D. Linear and Nonlinear Shear Rheology of a Marginally Entangled Ring Polymer. *Macromolecules* **2016**, *49*, 1444−1453.
(51) Struik, L. C. E.; Schwarzl, F. R. Conversion of Dynamic into Transient Properties, and Vice Versa. *Rheol. Acta* **1969**, *8*, 134−141.
(52) Larson, R. G.; Sridhar, T.; Leal, L. G.; McKinley, G. H.; Likhtman, A. E.; McLeish, T. C. B. Definitions of Entanglement Spacing and Time Constants in the Tube Model. *J. Rheol.* **2003**, *47*, 809−818.
(53) Matsumiya, Y.; Watanabe, H. Entanglement-Loosening Dynamics Resolved Through Comparison of Dielectric and Viscoelastic Data of Type-A Polymers: A Review. *Rubber Chem. Technol.* **2020**, *93*, 22−62.
(54) Hawke, L. G. D.; Ahmadi, M.; Goldansaz, H.; van Ruymbeke, E. Viscoelastic Properties of Linear Associating Poly (n-Butyl Acrylate) Chains. *J. Rheol.* **2016**, *60*, 297−310.
(55) Milner, S. T.; McLeish, T. C. B. Arm-Length Dependence of Stress Relaxation in Star Polymer Melts. *Macromolecules* **1998**, *31*, 7479−7482.
(56) Ball, R. C.; McLeish, T. C. B. Dynamic Dilution and the Viscosity of Star-Polymer Melts. *Macromolecules* **1989**, *22*, 1911−1913.
(57) Ferry, J. D. *Viscoelastic Properties of Polymers*, 3rd ed.; Wiley: New York, 1980.
(58) Walsh, D.; Zoller, P. *Standard Pressure Volume Temperature Data for Polymers*; CRC Press, 1995.
(59) Liu, C.-Y.; He, J.; Keunings, R.; Bailly, C. New Linearized Relation for the Universal Viscosity−Temperature Behavior of Polymer Melts. *Macromolecules* **2006**, *39*, 8867−8869.
(60) Fox, T. G.; Flory, P. J. Second-Order Transition Temperatures and Related Properties of Polystyrene. I. Influence of Molecular Weight. *J. Appl. Phys.* **1950**, *21*, 581−591.
(61) Fox, T. G. Influence of Diluent and of Copolymer Composition on the Glass Temperature of a Polymer System. *Bull. Am. Phys. Soc.* **1956**, *1*, 123.

https://doi.org/10.1021/acs.macromol.1c01329
Macromolecules 2021, 54, 11047−11060